Astron. Astrophys. 342, 524–530 (1999)

ASTRONOMY AND ASTROPHYSICS

HR 1817: the EUV properties of an active F dwarf

M. Mathioudakis[1] **and D.J. Mullan**[2]

[1] Department of Pure and Applied Physics, Queens University of Belfast, Belfast BT7 1NN, Ireland (e-mail: M.Mathioudakis@queens-belfast.ac.uk)
[2] Bartol Research Institute, University of Delaware, Newark, DE 19716, USA (e-mail: mullan@bartol.udel.edu)

Received 19 June 1998 / Accepted 28 September 1998

Abstract. We examine the coronal properties of the active F dwarf HR 1817. Photometric observations with EUVE show that the source is in a near-continuous state of flare-like activity. Using IUE and EUVE spectroscopic observations we construct the emission measure distribution in the 10^4–$10^{7.2}$ K temperature range. These observations reveal a hot corona and activity levels similar to those of RS CVn binaries. Based on Fe XXI line ratios we derive an upper limit of $10^{11.7}$ cm^{-3} for the coronal density of HR 1817 and a magnetic field strength of B$\leq$ 160 Gauss. A comparison of the EUVE spectroscopic observations with synthetic spectra derived from ASCA and ROSAT fits, shows that optimal agreement is obtained for fits with subsolar metal abundances. The reduced metal abundances increase the radiative losses significantly at temperatures above $10^{6.5}$ K where Fe is no longer the dominant radiative cooling agent.

Key words: X-rays: stars – ultraviolet: stars – stars: late-type – stars: individual: HR 1817 – stars: coronae – stars: activity

1. Introduction

The well established relations between rotation and spectral type in main sequence stars have shown that F dwarfs occupy a region in the H-R diagram where there is a sharp transition from high to low rotational velocities. Since the onset of surface convection takes place in late A – early F stars, this is also the mass range where chromospheric and coronal emission begins to appear. The rotational velocities of F0-F5 dwarfs in the Hyades and Pleiades are very similar, thus indicating that early F dwarfs do not undergo significant main sequence spindown (Stauffer 1995). The positive correlation between rotation and coronal X-ray emission which is such a prominent feature of cool stars disappears among stars with spectral types of dF5 and earlier (Walter 1983). These results may suggest that chromospheric and coronal emission in spectral types earlier than F5 may *not* be due to the same physical processes as those which are at work in cooler stars. However, in a recent paper Randich et al. (1996) have shown that the X-ray emission from early F stars in the α Per cluster, shows some correlation with the Rossby number. This result implies that the dependence of the emission on rotational velocity, is more pronounced in later spectral types because the convective turnover time is nearly constant over a large spectral range.

As regards stars later than dF5, it is widely believed (based on a solar analogy) that strong chromospheric and coronal emissions originate in large scale magnetic fields. According to this scenario, the positive correlation which is observed between rotation and coronal emission in cool stars is interpreted as evidence for large-scale dynamo operation inside the star (e.g. in the shear layer which separates the convective envelope from the radiative interior). The clearest evidence that a dynamo is at work in cool stars is the existence of a strong correlation between the magnetic moment μ of a star and its rotational angular momentum L, with a slope which is clearly different from the value +0.6: the latter is typical of objects where the magnetic and rotational properties are completely *uncorrelated* (Arge et al. 1995). In contrast to the cool star case, when data from warm and hot stars are compiled (with spectral type A9 and earlier), the slope of the μ *versus* L plot is close to +0.6 (Arge et al. 1995). This suggests that magnetism and rotation are *not* correlated in warm and hot stars. The lack of this correlation is probably the basic physical reason for the fact that there is no empirical correlation between rotational properties and chromospheric/coronal emission among these stars (Walter 1983).

Since rotation and chromospheric/coronal emission are *not* strongly correlated in warm stars, the origin of these emissions may be quite distinct from those in the Sun and cool stars. Suggestions which have been made to explain the warm star emissions include a turbulent magnetic field (Durney et al. 1993) and acoustic generation in convective turbulence (Mullan & Cheng 1994). In the turbulent magnetic dynamo scenario, the disappearance of observational correlations (Walter 1983) is explained by the fact that the turbulent velocity field is only weakly dependent on rotation. In the acoustic scenario, acoustic power emission is expected to be essentially spherically symmetric: thus, there should be no correlation between chromospheric/coronal emission and rotation, consistent with the data (Walter 1983).

The Extreme Ultraviolet Explorer (EUVE) has opened a new era in the study of stellar transition regions and coronae. The greatest capability of EUVE is through its spectroscopy which

Send offprint requests to: M. Mathioudakis

allows the observation of individual coronal lines formed in the 10^5 to $10^{7.2}$ K temperature range. The line to continuum ratios, elemental abundances and electron densities of the multitemperature stellar corona can therefore be studied (see for example Dupree et al. 1993, Griffiths & Jordan 1998). With EUVE, the assessment of atomic data in this relatively unexplored region of the electromagnetic spectrum has also become possible (Keenan 1996).

HR 1817(=HD 35850) is a dF8/9 star at a distance of 24 pc. It is a bright object (V=6.35) with absolute visual magnitude M_V = 4.45, i.e. only slightly more luminous than the Sun. The luminosity of HR 1817 is $L_* = 5 \times 10^{33}$ ergs s^{-1}, but the strength of the chromospheric/coronal emissions from HR 1817 indicates that its activity level is much higher than in the Sun. As a quantitative indication of the high level of activity in HR 1817, we note that with an X-ray luminosity of log $L_X = 30.2$ (Tagliaferri et al. 1997; hereafter T97), the coronal radiative output is at a level of $10^{-3.5}$ times the star's luminosity. This high level of coronal heating efficiency is close to the uppermost ("saturated") level of stellar activity among F8-G5 dwarfs (Walter 1983)

Despite the high level of activity in HR 1817, very few studies exist on this object to date. It was discovered as a serendipitous source in EXOSAT X-ray images and follow up optical spectroscopy revealed a large rotation rate ($vsini = 50$ km s^{-1}) (Tagliaferri et al. 1994; hereafter T94). Although in subsequent analysis, we will have occasion to compare our results with those obtained for certain RS CVn binaries, it is not yet established definitively that HR 1817 is in this class: spectroscopic data demonstrate that the radial velocity of HR 1817 is invariant (T94). Thus, if HR 1817 *is* an RS CVn system, i.e. if it is a binary, and the F star is tidally locked to the orbit, then the orbital plane must be very close to the plane of the sky in order to explain the constancy of the radial velocity. But if the system is viewed pole-on, how can the rotational broadening of a tidally locked component be as large as 50 km s^{-1}? We note that since the radius of HR 1817 is comparable to solar, a rotational velocity of 50 km s^{-1} corresponds to a rotation period of almost exactly 1 day: perhaps the lack of radial velocity variations is an effect of observing the system at the same phase of its orbit on successive nights.

The optical spectrum contains a strong Li I 6708 Å implying an abundance of log N(Li)=3.2 (T94). This high Li abundance, in combination with strong X-ray luminosity and fast rotational velocity, suggests that HR 1817 is a young star with an age similar to that of the Pleiades. Since the vast majority of stars within 25 pc are older than the Pleiades, it is possible that HR 1817 is a runaway object from a young cluster or a star forming region perhaps similar to HD 17925 (Cayrel de Strobel & Cayrel 1989). Because of the fast rotation, and the spectral type of F8/9, a solar type dynamo is expected to be in operation in HR 1817.

In a recent paper T97 have presented a thorough investigation of the X-ray emission of HR 1817 based on ASCA and ROSAT observations. In this paper we focus on the ultraviolet and extreme ultraviolet properties of HR 1817. One of our aims is to determine if analysis of EUV and UV data is consistent with analysis of the X-ray data.

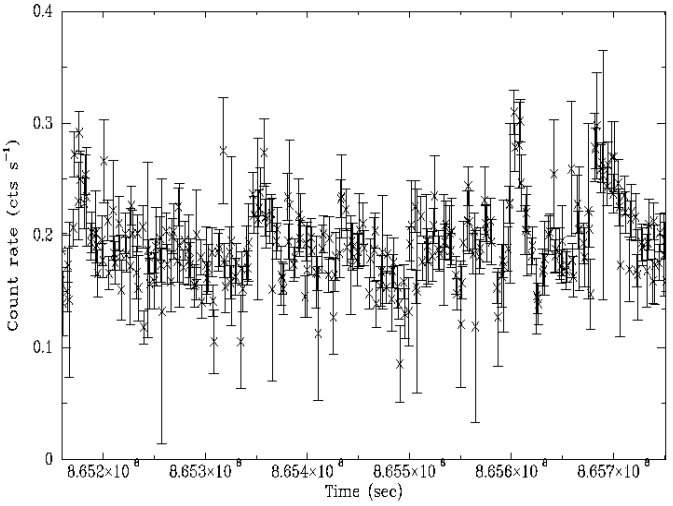

Fig. 1. The Deep Survey Lex/B (60–200 Å) light-curve of HR 1817. The time is given in seconds since JD 2440000.5

2. EUVE observations and data reduction

HR 1817 was observed with EUVE as part of a Guest Observer program from 08:15 October 23 1995 to 07:20 October 30 1995. The observations were carried out in a continuous pointing mode during 105 EUVE orbits. Each orbit lasts for $\approx$ 90 minutes and useful data are collected only during orbital night. Orbital night lasts for $\approx$ 1700 s, hence giving a total exposure time of $\approx$178,000 s. The observations were carried out with the Deep Survey/Spectrometer (DS/S) instrumental setup. The telescope used in this setup is aligned along the satellite spin axis and is divided into six equal segments. Three of the segments provide light for the DS instrument and the remaining three provide light for the spectrometers (Bowyer & Malina 1991). Each photon detected by EUVE is tagged with the time, detector number and detector coordinates.

2.1. EUV photometry – deep survey

The DS is a broad band imaging detector with three filter sections. The center section has a Lex/B filter (60–200 Å) with two segments of Al/C (170–360 Å) on either side (Bowyer et al. 1994). In the continuous pointing mode the source remains in the Lex/B filter throughout the observation. The EUVE data were corrected for the instrumental effects of dead-time and primbsching using the EUV software *egocs* 1.6 and *egodata* 1.12 (Abbott et al. 1996). Further analysis was performed with the PROS X-ray package available on IRAF. Source counts were determined in a circle centered on the position of the source, which was sufficiently large to encompass the instrument point spread function. Background counts were determined in an annulus centered in the same position. The data were binned into 1000 second time bins. The mean count rate is about 0.2 cnts s^{-1}, although variability relative to the mean level is obvious. A time-line of the DS observations is presented in Fig. 1.

HR 1817 was detected during the EUVE all sky survey with 0.105$\pm$0.01 cnt s^{-1} in Lex/B and 0.037$\pm$0.01 cnt s^{-1} in

Al/Ti/C (Bowyer et al. 1994). Accounting for the fact that the DS Lex/B is a factor of two more sensitive than the scanner Lex/B, the agreement between the all-sky survey and our observations is very good. Assuming a single temperature coronal model of log T = 7.0 and based on the conversion factors presented by Mitrou et al. (1997), we derive luminosities of $L_{Lex/B} \approx 2 \times 10^{29}$ erg s^{-1} and $L_{Al/Ti/C} \approx 1.0 \times 10^{29}$ erg s^{-1}. The integrated flux of the EUVE SW spectrograph agrees within 30% with the Lex/B luminosity. A further comparison of the EUVE count rates in both filters with the ROSAT/WFC S1 and S2 filters shows no evidence for long-term coronal variability in this source (Pye et al. 1995).

From Fig. 1 we see that HR 1817 was in a near-continuous state of variability throughout the EUVE observations. We investigated the variability quantitatively by using the Kolmogorov-Smirnov (K-S) and Cramer-von Mises (CvM) tests on IRAF. In both tests, we compare the observed cumulative distribution function of photon arrival times with a model expected from a constant source. Both tests indicate that variability is indeed detected at the 99% confidence level. The variations (flares?) occur on timescales of a few hours with peak count rates at $\approx$ 50% above that of the 'quiescent' state. The total integrated energies of these flare-like events are in the range of 5×10^{32}–2×10^{33} ergs.

2.2. EUV spectroscopy

The spectroscopic capability of EUVE consists of three spectrometers, at short (SW: 70-190 Å), medium (MW: 140-380 Å), and long wavelengths (LW: 280–760 Å), with a resolving power in the range of $\frac{\lambda}{\Delta\lambda} \sim 150 - 350$. The rms errors in wavelength are 0.11 Å in the SW, 0.13 Å in the MW and 0.25 Å in the LW corresponding to 0.22,0.13 and 0.13 resolution elements respectively (Abbott et al. 1996). The flare-like events detected by the DS are not sufficiently bright for their individual spectra to be determined: we are limited to extracting an average spectrum. To do this, we used the standard EUV package available on IRAF. Emission line fluxes were determined by fitting gaussians to the observed line profiles. The line width at half maximum was determined from the fit and in all cases was found to agree with the instrumental resolution. A very weak "continuum" contribution was subtracted in the SW spectrum. There is no evidence for a continuum in the MW and LW spectra and the line fluxes were measured from the zero flux level. The interstellar medium can be a major source of uncertainty in the line fluxes, particularly at longer wavelengths. The lines that are mostly affected are Fe XVI at 335.41 Å and 360.80 Å with a theoretical ratio of 2:1 (Brickhouse et al. 1995). A mean hydrogen density of 0.05 cm^{-3} (Zombeck 1990) would lead to a hydrogen column density of log N_h = 18.6 cm^{-2} at the distance of HR 1817. However, this N_h appears to be too high to reproduce the observed Fe XVI line ratio. A lower value in the range of log N_h = 18.0–18.3 cm^{-2} appears more appropriate. A column density log N_h = 18.3 cm^{-2} was chosen in the present study. (This value is consistent with the database of N_h presented by Fruscione et al. 1994.) If we were to choose log N_h = 18.0 cm^{-2}, this would decrease the attenuation factor by a factor of 2.3 at 360 Å while the effect in the SW spectrum would be less than 10%. The spectra were corrected for interstellar extinction using the hydrogen, helium and ionized helium cross sections compiled by Rumph et al. (1994). The SW and MW spectra are shown in Fig. 2 whereas fluxes for the strongest EUV lines are given in Table 1. The Fe XVI lines at 335.41 Å, 360.80 Å and He II 304 line, are detected in both the medium and long wavelength spectrometers; the fluxes from the two spectrometers agree to within 30%.

Table 1. UV and EUV line fluxes of HR 1817. The fluxes have been corrected for interstellar attenuation and are given in units of $10^{-13}\,erg\,cm^{-2}s^{-1}$.

Ion	λ_{theo}	Line flux
Fe XVIII	93.92	1.1
Fe XIX	108.37	1.4
Fe XXII	117.17	0.6
Fe XX	118.66	0.4
Fe XX	121.83	0.7
Fe XXI	128.73	1.7
Fe XX/Fe XXIII	132.85	3.5
Fe XXII	135.78	0.8
Fe XXIV	192.04	$1.5UL$
Fe XV	284.15	1.6
[1]He II	304	15.9
[1]Fe XVI	335.41	6.4
[1]Fe XVI	360.8	3.8
C III	1176	3.9
N V	1238.8/1242.8	1.1
C II	1334.53/1335.71	5.8
Si IV	1393.8	3.3
Si IV	1402.8	2.3
C IV	1548.2/1550.8	9.1
He II	1640.7	3.3

[1] Flux determined from the EUVE medium wavelength spectrum.

2.3. UV spectroscopy

HR 1817 was observed by IUE in the low resolution mode in November 1995 and February 1996. The IUE log is given in Table 2, whereas the SWP and LWP spectra are shown in Fig. 3. Strong emission lines of C IV and Si IV are easily visible in the spectrum: these lines are characteristic of highly active stars. Also apparent is a strong photospheric continuum rising from 1700 Å towards longer wavelengths. Mean fluxes of the most prominent lines in the SWP spectra are listed in Table 1.

In the LWP spectra, the photospheric continuum is dominant. There is a broad absorption feature due to Mg II around 2800 Å but the chromospheric emission core of this line is not detected. This non-detection is somewhat surprising in a star with such a high level of activity. We attribute our non-detection of the Mg II chromospheric emission to a combination of the strong photospheric continuum and low resolution: the latter can "wash out" weak emission features.

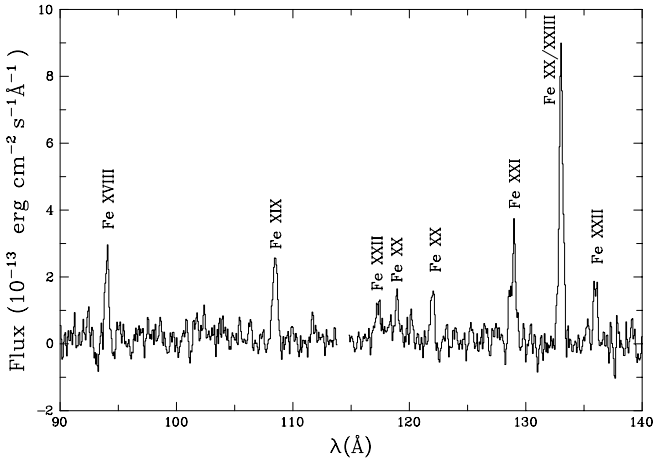

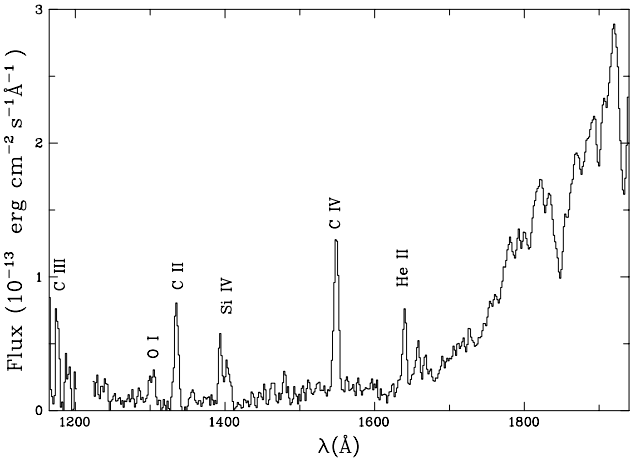

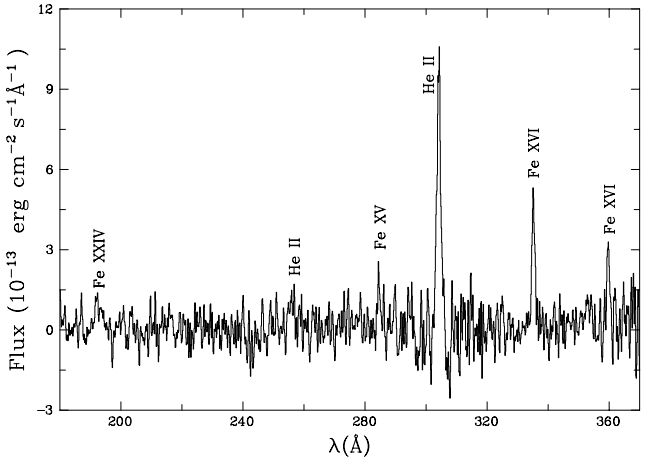

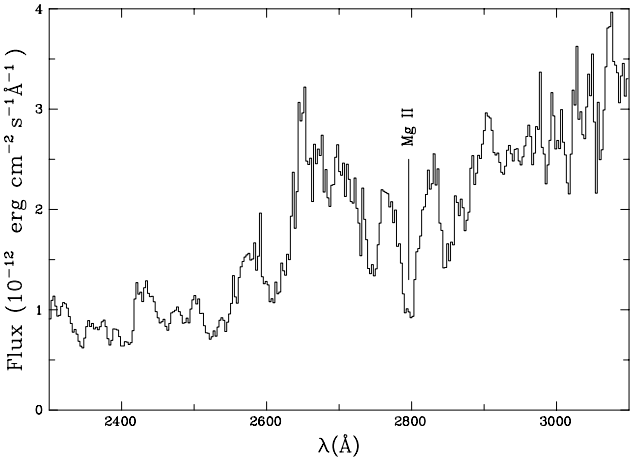

Fig. 2. The EUVE short and medium wavelength spectra of HR 1817.

Fig. 3. The IUE spectra of HR 1817. The strongest lines in SWP and the position where the Mg II emission core is expected in the LWP are noted.

Table 2. The IUE observation log for HR 1817.

Image No	Date	UT start	Exp time sec
LWP 31672	8 November 1995	20:58	600
SWP 56169	8 November 1995	21:14	2400
LWP 31980	12 February 1996	19:46	600
SWP 56801	12 February 1996	20:21	2400

3. Results and discussion

3.1. Comparison with ASCA & ROSAT observations

In a recent paper T97 have presented a thorough investigation of the X-ray properties of HR 1817. They perform fits to ASCA Solid State Imaging Spectrometers (SIS) and Gas Imaging Spectrometer (GIS) as well as ROSAT Position Sensitive Proportional Counter (PSPC) observations and derive the temperature, emission measure and metal abundances of the corona. The fits which they present assume that the coronal temperatures are limited to either one, two, or three values: we refer to these as 1T, 2T and 3T fits, respectively. An examination of the parameters of the fits obtained by T97 shows that the plasma that dominates the ASCA and ROSAT spectral ranges is also expected to emit in the EUV. To carry out a comparison with the results presented here we have proceeded as follows. The emission measure, temperature and coronal abundances derived by T97 have been used to generate model spectra. The spectra were generated with the XSPEC package, using the Mewe et al. (1986,1996) line emissivities also known as *mekal*. The spectra were then folded through the EUVE spectrometer effective areas using the EUV task *specmod* available in IRAF. Poisson noise has also been added to the model spectra. We emphasize that the Fe XXIV line at 192.04 Å has an ionization fraction that peaks at $10^{7.2}$ K: this is the *hottest* line that can be detected in the EUVE wavelength range.

In models of the HR 1817 corona which T97 obtained by assuming that the abundances are equal to solar (Z=1), the 2T and 3T fits to the ASCA SIS spectra include strong components in the $10^{6.7}$–$10^{7.4}$ K temperature range: however, the Fe XXIV (192.04 Å) line flux predicted for this component is too strong to be consistent with our EUVE spectra. Removing the restriction on abundances, T97 examine cases in which abundances are sub-solar (Z$<$1). They find that the best values for the reduced χ^2 are obtained with a 2T fit to the SIS1 detector using Z=0.32. However, this fit does not reproduce the EUVE observations: it

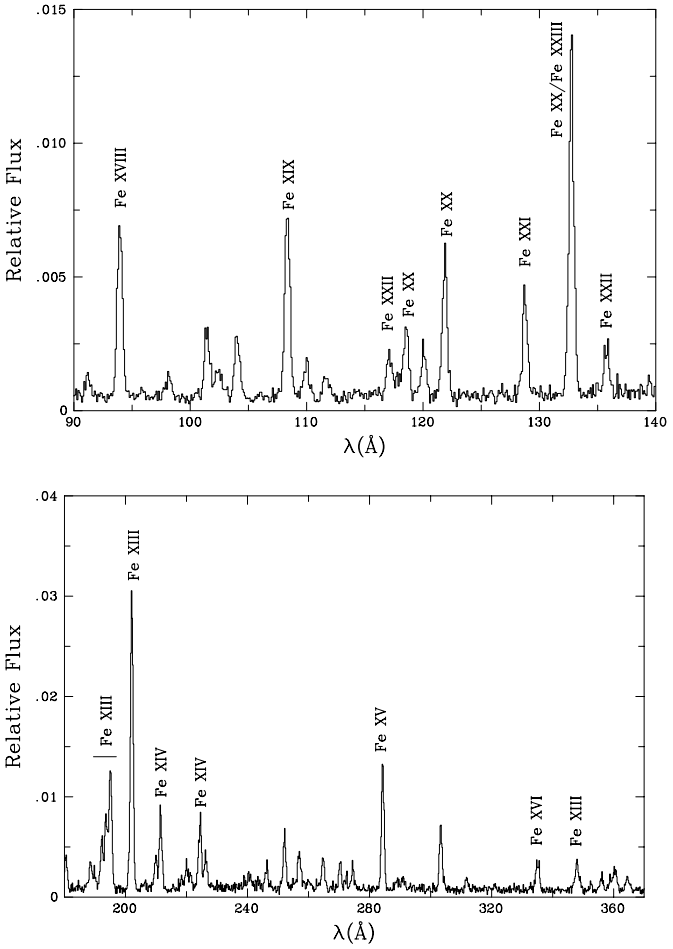

Fig. 4. Synthetic short and medium wavelength EUV spectra of HR 1817. The spectra have been constructed from a simultaneous fit to the ASCA SIS0, GIS2 and ROSAT PSPC detectors with solar abundances (Z=1). A comparison with the EUVE spectra of the source (Fig. 2) shows that the temperature component at $10^{6.2}$ K produces strong Fe XIII–Fe XV lines which are not seen in the observed spectrum.

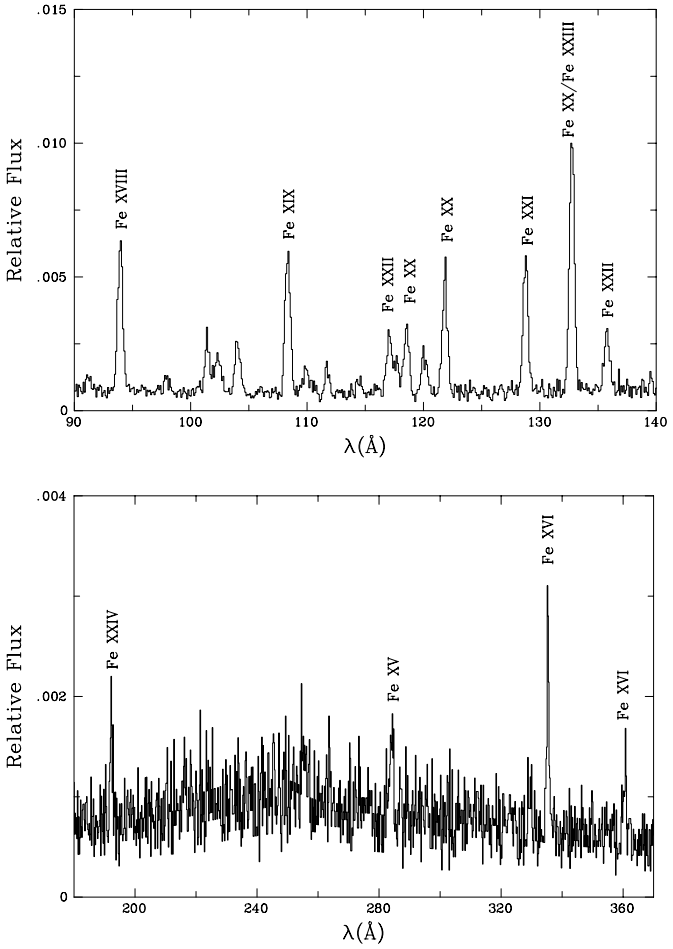

Fig. 5. Synthetic short and medium wavelength EUV spectra of HR 1817. The spectra have been constructed from a simultaneous fit to the ASCA SIS0, GIS2 and ROSAT PSPC detectors with sub-solar abundances Z=0.34. A very good agreement with the observed spectra is evident.

still over-predicts the Fe XXIV flux relative to the cooler lines. Since the calibration of the SIS1 detector is not known as well as that of SIS0, this might be due to an incorrect normalization factor of the high temperature component. The model of T97 which agrees best with EUVE is a 2T model to the SIS0 detector using Z=0.18.

Although the best values for the reduced χ^2 are produced by the GIS fits, the derived parameters in all cases predict unacceptable EUV spectra. The 2T models with solar abundances over-predict the high temperature components; the same conclusion applies to the 1T models with sub-solar abundance. We attribute this inconsistency to the low spectral resolution of the GIS detector. The ROSAT PSPC 2T model with solar abundances produce a very strong component at $10^{6.3}$ K. The predicted line fluxes of Fe XIII–Fe XV, are too strong compared with the observed MW spectra. The EUV spectra are correctly reproduced with the PSPC 2T model with sub-solar abundances.

The same conclusion is reached from the simultaneous fit to PSPC, SIS0 and GIS2. Note that SIS0 and GIS2 are the best calibrated ASCA detectors and SIS0 is the one with the highest resolution. The synthetic spectra from these fits are shown in Figs. 4 and 5 where the strongest lines are identified. The solution based on solar abundance Z=1 produces strong Fe XIII–Fe XV lines and is therefore unacceptable. However, when metal abundances were allowed to vary in overall amount (but keeping the solar proportion among elements), a good fit is obtained for Z=0.34. This fit also produces an excellent agreement with the EUVE observations (Fig. 5). We therefore conclude that the best coronal models of HR 1817 published by T97, are consistent with the EUV observations.

3.2. The emission measure distribution

The EUVE spectrum of HR 1817 is dominated by Fe XV–Fe XXIII. The flux of an optically thin coronal line depends on the elemental abundance, the ionization fraction, the relative population of the lower level and the excitation rate. Here we

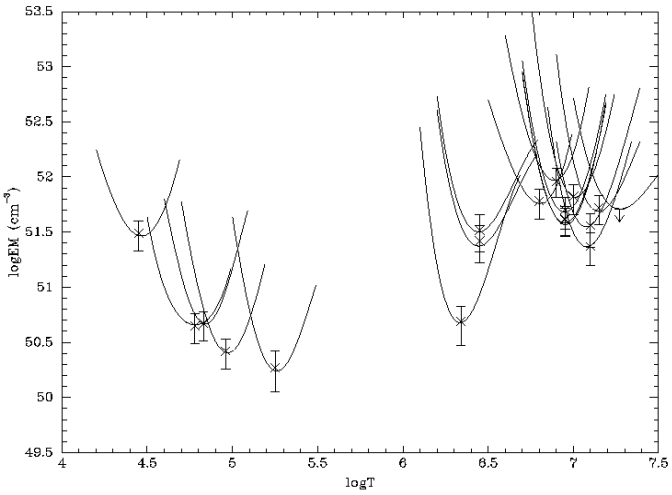

Fig. 6. The emission measure distribution of HR 1817. The line contribution functions are also plotted.

use the Brickhouse et al. (1995) iron line emissivities which have been calculated with the Arnaud & Raymond (1992) ionization balance, an Fe abundance of 7.6 and an electron density of $N_e = 10^{10}$ cm^{-3}. If the Arnaud & Rothenflug (1985) ionization balance was to be used instead, the Fe peak ionization fraction would be shifted to slightly lower temperatures ($\approx$ 0.1dex). A detailed discussion of the two ionization balances is given by Laming et al. (1995). For the UV lines we use the Doyle & Keenan (1992) line emissivities for an electron pressure of P_e = 10^{16} cm^{-3} K. The biggest effect of the pressure/density on the emissivities is seen for Si IV where they can vary by as much as 45%, whereas the remaining UV lines vary between 15%-35% in the 10^{14}–$10^{17.5}$ cm^{-3} K pressure range. The volume emission measure $EM(T)$ is then given by the relation:

$$EM(T) = 4\pi d^2 \frac{F_{obs}}{\epsilon} \quad (1)$$

where d is the distance to the object, F_{obs} the observed flux and ϵ the corresponding line emissivity. The emission measure distribution of HR 1817 is presented in Fig. 6. The accumulated error from the uncertainty in the line fluxes and a 30% uncertainty in the line emissivities is also plotted.

The line at 132.85 Å is due to an Fe XX/Fe XXIII blend. If we assume a constant emission measure, 70% of the flux is attributed to Fe XXIII and 30% to Fe XX. However, this assumption may overestimate the emission measure of Fe XXIII and therefore cause a significant dispersion in the values of the emission measure at the temperature of $10^{7.1}$ K. The Fe XXII line at 117.17 Å is possibly blended with Fe XXI 117.51 Å. For densities below 10^{12} cm^{-3}, which are applicable for HR 1817 (see below), the contribution of Fe XXII is $\approx$20%. Since the values of the emission measure are quite low at temperatures below $10^{6.2}$ K, the remaining EUV lines have no significant blends.

The data points in Fig. 6 suggest that in the temperature range log T = 5.2-6.9, the $EM(T)$ curve has a positive slope. Assuming $EM \sim T^b$, a lower limit to the value of the slope b can be obtained by connecting the data point marked by a cross at log T = 5.2 to the point at log T = 6.9: the lower limit case has b = 1.0$\pm$0.2. If, instead of using the data point at log T = 5.2, we were to use the data point at log T = 6.3, and connect it to the point at log T = 6.9, the slope would be much steeper: $b \approx$ 2.0. We note that these estimates of b in our results for HR 1817 overlap with some of the estimates of b which occur in various solar features: b = 0.9 (in coronal hole network), b = 2.1 (in quiet Sun cell), and b = 3.1 (flares) (Raymond & Doyle 1981). Considerations of energy balance have led Jordan (1980) to suggest that b might be limited for physical reasons to values around 1.5, although Raymond & Doyle (1981) refer to this suggestion as "controversial". Even in the case of the Sun, where differences in the slope are observed in features of different magnetic topology, attempts to identify specific contributors to different energy balance equations have not led to any definitive conclusions (Raymond & Doyle 1981). By means of simulations, it may eventually be possible to interpret the observed $EM(T)$ in terms of a heating function, or in terms of loop geometry, although as Van den Oord et al. (1996) has stressed, this "is a delicate process".

The radiative losses of the corona can be computed as the product of the emission measure with the radiative loss function Λ(T) of an optically thin plasma. The radiative losses provide a lower limit to the coronal heating requirements. Iron becomes an increasingly important contributor to the radiative loss function for temperatures above 10^5 K and dominates between $10^{5.7}$–$10^{6.5}$ K (Cook et al. 1989). Radiative losses from bremsstrahlung radiation become important at higher temperatures. If we use the Meyer (1985) solar coronal abundances for HR 1817, we estimate radiative losses of 10^{30} erg s^{-1} over the 10^6–10^7 K temperature range. However, as we have already pointed out there is strong evidence that the Fe abundance in the corona of HR 1817 is significantly lower than the solar. We have therefore used the Cook et al. (1989) radiative loss function scaled appropriately for a reduced Fe abundance of 0.25 of the solar value, to recompute the radiative losses. The reduced Fe abundance will increase the emission measure and decrease the radiative loss function. The reduced abundance will therefore cause little differences in the radiative losses in the temperature range where Λ(T) is dominated by Fe; however, differences as much as a factor of 4 are found in higher temperatures as losses from bremsstrahlung radiation become important.

3.3. An estimate of the electron density

The EUVE spectral range offers several line ratios that can be used as density diagnostics (Doschek 1991). The coronal spectrum of HR 1817 is dominated by the highest ionization stages of iron. We have attempted to estimate the electron density in HR 1817 using Fe XXI, a good density diagnostics in high density plasmas ($10^{11.5}$–10^{15} cm^{-3}) (Keenan 1996). The Fe XXI line ratios applicable in this case are R_1=(102.22 Å/128.73 Å), R_2=(121.22 Å)/(128.73 Å) and R_3=(142.15 Å)/128.73 Å). The 128.73 Å line is one of the strongest in the spectrum whereas only upper limits can be determined for the flux of the lines at 102.22 Å 121.22 Å and 142.15 Å indicating that $R_1 \leq 0.20$,

$R_2 \leq 0.1$ and $R_3 \leq 0.25$. The line ratios were checked against the theoretical values of Brickhouse et al. (1995) and Dere et al. (1996) (CHIANTI database) and upper limits to the electron densities of $n_e \leq 11.7$, $n_e \leq 12.0$, $n_e \leq 12.7\,cm^{-3}$ were derived from R_1, R_2 and R_3 respectively. Griffiths & Jordan (1998) estimate the electron density in the corona of three RS CVn binaries by fitting the emission measure of the Fe XXI 128.73 Å line to the emission measure distribution as determined from lines of other ions. However, given the dispersion of the values of the emission measure we will not be using this method in the present study. Our electron density is in agreement with the Griffiths & Jordan (1998) values but is up to factor of 30 lower than the high values quoted for the corona of Capella. We emphasize however, that in the case of Capella there is a large inconsistency in the values of n_e derived from different Fe XXI line ratios (Dupree et al. 1993). The electron density combined with an emission measure of 5×10^{51} cm^{-3} at 10^7 K implies that the volume of the emitting plasma is greater than 2×10^{28} cm^3. If we assume that the coronal plasma is distributed in semicircular loops with a cross-sectional diameter $\approx 20\%$ of the footpoint separation, the radius R of the loop is given by

$$R \geq 3.7 \times 10^9 n^{-\frac{1}{3}} \quad (2)$$

where R is in cm and n is the number of loops. Although we only have an upper limit to the density, we point out that if n_e in the corona of HR 1817 has values of the order of 10^{12} cm^{-3} this would imply that the coronal structures are relative compact, similar to those of RS CVn binaries (Van den Oord et al. 1996).

The density estimate from Fe XXI allows us to derive an upper limit for the pressure of $p \leq 10^3$ dyne cm^{-2} at a temperature of 10^7 K. The confinement of the gas therefore requires a magnetic field of B$\leq$ 160 Gauss.

4. Conclusions

In the present paper we have used EUVE observations to examine the coronal properties of the F8/9 dwarf HR 1817. The source was in a near-continuous state of low amplitude variability (flaring?) throughout the EUVE observations. For individual variability events (flares?), the integrated energies amounted to some 2×10^{33} ergs in the EUVE Lex/B band (60–200 Å). We have combined EUVE and IUE spectroscopic observations to construct the emission measure distribution over the $10^{4.3}$–$10^{7.2}$ K temperature range. The EUV spectrum is dominated by hot coronal lines of Fe XV–Fe XXIII and the emission measure distribution peaks at a temperature of 10^7 K. The non-detection of the Fe XXI line at 102.22 Å only allows us to place an upper limit of log $n_e \leq 11.7\,cm^{-3}$ to the electron density and to the coronal magnetic field strength B$\leq$ 160 Gauss. The activity levels of HR 1817 are comparable to active RS CVn binaries, although there is no spectroscopic evidence at present to suggest that HR 1817 is in fact a binary. We have used the temperature, emission measure and abundances derived from the ASCA and ROSAT observations of T97, to construct synthetic spectra which we then compared with the observations. We found that in most cases the models with solar abundances produce a strong low temperature component at $10^{6.2}$ K. This temperature component produces strong Fe XIII–Fe XV which are not seen in the observed spectrum. In fact the only models that produce good agreement are those with abundances of 0.2-0.3 the solar value. The new Fe abundance increases the coronal radiative losses particularly at temperatures above $10^{6.5}$ K where bremsstrahlung radiation begins to dominate the radiative loss function.

Acknowledgements. This work has been supported by an EUVE Guest Observer program.

References

Abbott M.J., Boyd W.T., Jelinsky P., et al., 1996, ApJS 107, 451
Arge C.N., Mullan D.J., Dolginov A.Z., 1995, ApJ 443, 795
Arnaud M., Raymond J., 1992, ApJ 398, 394
Arnaud M., Rothenflug R., 1985, A&AS 60, 425
Bowyer S., Malina R.F., 1991, In: 397
Bowyer S., Lieu R., Lampton M., et al., 1994, ApJS 93, 569
Brickhouse N.S., Raymond J.C., Smith W.C., 1995, ApJS 97, 551
Cayrel de Strobel G., Cayrel R., 1989, A&A 211, 324
Cook J.W., Cheng C-C., Jacobs V.L., Antiochos S.K., 1989, ApJ 338, 1176
Dere K.P., Landi E., Mason H.E., Monsignori-Fossi B.C., Young P.R., 1997, A&AS 125, 149
Doschek G.A., 1991, In: Malina R.F., Bowyer S. (eds.) Extreme Ultraviolet Astronomy. Pergamon Press, p. 94
Doyle J.G., Keenan F.P., 1992, A&A 264, 173
Dupree A.K., Brickhouse N.S., Doschek G.A., Green J.C., Raymond J.C., 1993, ApJ 418, L41
Durney B.R., De Young D.S., Roxburgh I.W., 1993, Solar Physics 145, 207
Fruscione A., Hawkins I., Jelinsky P., Wiercigroch A., 1994, ApJS 94, 127
Griffiths N.W., Jordan C., 1998, ApJ 497, 883
Jordan C., 1980, A&A 86, 355
Keenan F.P., 1996, Space Sci. Rev. 75, 537
Laming J.M., Drake J.J., Widing K.G., 1995, ApJ 443, 416
Mewe R., Lemen J.R., van den Oord G.H.J., 1986, A&AS 65, 511
Mewe R., Kaastra J.L., Liedahl D.A., 1996, Legacy. The Journal of HEASARC 6, 17
Meyer J-P., 1985, ApJS 57, 172
Mitrou C.K., Mathioudakis M., Doyle J.G., Antonopoulou E., 1997, A&A 317, 776
Mullan D.J., Cheng Q.Q., 1994, ApJ 435, 435
Pye J.P., McGale P.A., Allan D.J., et al., 1995, MNRAS 274, 1165
Randich S., Schmitt J.H.M.M., Prosser C.F., Stauffer J.R., 1996, A&A 305, 785
Raymond J., Doyle J.G., 1981, ApJ 247, 686
Rumph T., Bowyer S., Vennes S., 1994, AJ 107, 2108
Stauffer J.R., 1995, In: Caillault J.P. (ed.) Cool Stars Stellar Systems and the Sun. ASP Conference Series Vol. 64, p. 163
Tagliaferri G., Cutispoto G., Pallavicini R., et al., 1994, A&A 285, 272 (T94)
Tagliaferri G., Covino S., Fleming T.A., et al., 1997, A&A 321, 850 (T97)
Van den Oord G.H.J., Schrijver C.J., Mewe R., Kaastra J.S., 1996, In: Cool Stars, Stellar Systems, and the Sun. ASP Conference Series No. 109, p. 231
Walter F.M., 1983, ApJ 274, 794
Zombeck M.V., 1990, In: Handbook of Space Astronomy & Astrophysics. Cambridge University Press